

## Research Article

# Study on Mechanics-Based Cracking Resistance of Semiflexible Pavement Materials

Duanyi Wang, Xiayi Liang , Danning Li , Hehao Liang , and Huayang Yu 

*School of Civil Engineering and Transportation, South China University of Technology, Guangzhou 510641, China*

Correspondence should be addressed to Huayang Yu; [huayangyu@scut.edu.cn](mailto:huayangyu@scut.edu.cn)

Received 7 June 2018; Revised 10 September 2018; Accepted 31 October 2018; Published 21 November 2018

Guest Editor: Munir Nazzal

Copyright © 2018 Duanyi Wang et al. This is an open access article distributed under the Creative Commons Attribution License, which permits unrestricted use, distribution, and reproduction in any medium, provided the original work is properly cited.

Semiflexible mixture is a composite paving material combining the advantages of both asphalt and cement concrete materials. It consists of matrix asphalt skeleton and cement mortar. Due to the different volume characters between asphalt structure and cement mortar, stress concentration always happens in this semiflexible mixture, leading to internal cracking. The objective of this study is to alleviate the internal cracking concern of the semiflexible mixture by adjusting the material components. To this end, optimal material design and numerical simulation have been conducted. Matrix asphalt structures with four different air voids were incorporated with different dosages of cement mortar. The contraction strain and expansion strain of cement mortar as well as the indirect tensile strength of matrix asphalt structure were measured. The results were input into ABAQUS for numerical simulation. The results indicated that (1) the internal stress in this semiflexible mixture is mainly determined by the contraction of cement mortar, rather than expansion; (2) larger air void of matrix asphalt structure and less volumetric variation of cement mortar reduce the internal stress; (3) once the air void of matrix asphalt structure is decided, both maximum contraction and expansion deformations of cement mortar should meet specific requirement to ensure less internal cracking. This is a practical-ready paper that provides reference for the anticracking design of semiflexible pavement.

## 1. Introduction

Semiflexible pavement material is a composite pavement material, which consists of porous asphalt structure and cement mortar. The main advantages of semiflexible pavement include high carrying capacity, high wearing resistance, high shear resistance, high water stability, and driving comfort. Semiflexible pavement material has very bright application prospects and is suitable for intersection turner, gas station, parking, bus station, airport runways, and other sections [1–6]. However, the insufficient volume stability resulted from the defects in the material composition and structure of semiflexible pavement leads to frequent cracking. The cracks occurring in semiflexible pavement materials can be divided into three types based on their causes: fatigue cracking under the action of traffic load, temperature contraction cracking and dry contraction cracking caused by temperature and humidity variation, and reflection cracks of semirigid base cracking [7]. Fatigue crack

and reflection crack are mainly caused by traffic load. In addition, temperature contraction cracking and dry contraction crack result from the different volume stability of asphalt mixture matrix and cement mortar. The volume of cement mortar can be greatly changed when the water reaction period or ambient temperature varies greatly. Consequently, the volume deformation of the asphalt mixture matrix and cement mortar cannot be coordinated. This incoordination leads to the stress concentration in semiflexible pavement, which makes the pavement more prone to crack. Thus, internal stress control of semiflexible pavement is particularly critical for crack resistance.

The effects of asphalt, aggregate, and cement mortar on the volumetric stability and cracking resistance of semiflexible pavement were studied by Huang [7], who researched and developed an easy-to-pour small contraction deformation polymer cement mortar. Wang and Wu [8] evaluated the cracking resistance of semiflexible pavement materials based on the fracture toughness using the

J-integral theory and three-point bending semicircular beam test. Huang et al. [9] studied the cracking resistance of semiflexible pavement materials based on cement-emulsified asphalt mortar. At present, studies of the anticracking of semiflexible pavement have been mainly focused on controlling the volumetric stability of the cement mortar and the overall cracking resistance of semiflexible pavement materials. However, few researchers have mechanically studied the internal cracking resistance and anticrack design of semiflexible pavement. Therefore, to improve the cracking resistance of semiflexible pavement from the material composition, the control of the internal stress of the cement mortar and matrix asphalt mixture in semiflexible pavement is particularly critical. In other words, the prerequisite for the anticracking design of semiflexible pavement materials is that the expansion stress and contraction stress of the cement mortar must be lower than the ultimate tensile strength of the asphalt mixture matrix.

In this paper, the expansion strain and contraction strain of cement mortar and the matrix were determined firstly. The ultimate tensile strength of the asphalt mixture matrix was measured. Then digital images of semiflexible pavement cross section were collected using a CCD digital camera. The locations of the cement mortar, asphalt, aggregate, and voids were obtained using AutoCAD software. The finite element analysis method was employed for the mechanical analysis of the digital image results. Taking the internal stress peak as the control index, this paper put forward the standard of strain control of cement mortar, which can effectively control the cracking of semiflexible pavement materials.

## 2. Materials and Methods

**2.1. Materials.** The performance indicators of materials used to prepare the cement mortar and the matrix of semiflexible pavement are shown in Tables 1–4.

**2.2. The Expansion Strain and Contraction Strain of Cement Mortar.** The expansion strain and contraction strain of cement mortar are the main reasons for the internal stress in semiflexible pavement. In order to explore the anticracking performance of semiflexible pavement, this paper measured the maximum expansion strain and contraction strain of cement mortar.

Referring to “Explain for General Code of Asphalt Pavement Engineering” [10], the cement mortar fluidity, compressive strength, flexural strength, and amount of contraction were used as the evaluation index. Based on the orthogonal test method, taking water-cement ratio and dosage of mineral filler and sand as the influencing factors, the indoor relevant experimental study would be processed to measure the flow performance, bending resistance, and volume stability of cement mortar. Through the range analysis, the best mix ratio of cement mortar can be determined, which is shown in Table 5.

**2.2.1. The Expansion Strain of Cement Mortar.** It has been shown that the thermal expansion coefficient of cement

TABLE 1: Gradation of standard sand.

Sieve size (mm)	1.18	0.6	0.3	0.15	0.075	Content of clay (%)
Passing rate (%)	100	98.5	92.7	51.5	2.2	0.5

TABLE 2: Technical indexes of mineral filler.

Testing indexes	Expressway or first grade highway requirement	Other grade highway requirement	Value
Apparent relative density ( $\text{g}/\text{cm}^3$ )	$\geq 2.50$	$\geq 2.45$	2.761
Water content (%)	$\leq 1$	$\leq 1$	0.27
Hydrophilic coefficient (%)	$< 1$	$< 1$	0.33
Plasticity index	$\leq 4$	$\leq 4$	2.4

TABLE 3: Technical indexes of asphalt.

Testing indexes	Technical requirement	Value
Penetration 25°C, 100 g, 5 s, 0.1 mm	60–80	68
Softening point TR&B (°C) min	$\geq 46$	49.5
Ductility 5°C, 5 cm/min, cm	$> 15$	65
Ductility 15°C, 5 cm/min, cm	$\geq 100$	$> 100$
Solubility (%) min	$\geq 99.5$	99.6
Flash point (°C) min	$\geq 260$	285
Wax content (%)	$\leq 2.2$	1.8
Dynamic viscosity 60°C	$\geq 180$	215
	Quality change	$\pm 0.8$
Rotate the film to heat the test residue (163°C, 85 min)	Penetration ratio: 25°C	$\geq 61$
	Ductility: 10°C, cm/min	$\geq 6$
		25.2

TABLE 4: Technical indexes of aggregate.

Testing indexes	Value	Technical requirement
Crushing value (%)	11	$\leq 26$
Los Angeles wear value (%)	12	$\leq 28$
Stone polishing value (BPN)	55	$\geq 42$
Coarse aggregate ruggedness (%)	4	$\leq 12$
Coarse aggregate needle sheet content (%)	4	$\leq 15$
Sand equivalent (%)	53	$\leq 65$
Methylene blue value (g/kg)	1.1	$\leq 2.0$

TABLE 5: Optimal mix ratio of cement mortar.

Cement mortar indicators	Water-cement ratio	Dosage of mineral filler (%)	Dosage of sand (%)
Value	0.61–0.63	10	20

mortar is time-dependent, whose largest value is  $48 \mu\epsilon/^\circ\text{C}$  during the initial setting [11]. After the initial setting, the coefficient of thermal expansion decreases and reaches the lowest value of approximately  $11 \mu\epsilon/^\circ\text{C}$  during the final setting. As time goes by, the coefficient of thermal expansion will increase slowly to the second largest value of  $13.6 \mu\epsilon/^\circ\text{C}$  and will then gradually stabilize at  $13.1 \mu\epsilon/^\circ\text{C}$ . Therefore, the thermal expansion deformation becomes the largest when the cement mortar undergoes a hydration reaction. According to the actual project time, semiflexible pavement is generally constructed during the summer. Using the most unfavorable climatic conditions as a reference, the maximum surface temperature difference in Guangdong Province of China is about  $40^\circ\text{C}$  in summer, and the maximum expansion strain of cement mortar may be  $1.92 \times 10^{-3}$ .

**2.2.2. The Contraction Strain of Cement Mortar.** Contraction deformation of cement mortar can be divided into dry contraction, temperature contraction, plastic contraction, self-contraction (hardening contraction), and carbonation contraction. Among them, dry contraction is not only the most common deformation type of cement mortar but also the main reason for the cracking of materials [12]. In this paper, the maximum contraction strain of cement mortar is determined by a contraction test. According to the optimal mix ratio of cement mortar described in Table 5, a triple-test-molded dry contraction specimen with a standard size of  $25 \text{ mm} \times 25 \text{ mm} \times 250 \text{ mm}$  was created. After the specimen was formed, it was maintained for 24 hours in a curing room at a temperature of  $20 \pm 3^\circ\text{C}$  and a relative humidity of 98%. Then, the specimens were removed and their initial lengths were measured. The specimens were moved into a box with constant temperature and humidity ( $20 \pm 1^\circ\text{C}$  and relative humidity of  $50 \pm 3\%$ ). The contraction deformations of the cement mortar were measured at 1, 3, 7, 14, 28, 35, 60, 90, 120, 150, and 180 days. The average contraction strains were calculated, and the results of which are shown in Figure 1.

As shown in Figure 1, the average contraction strain of cement mortar increases with time and finally tends to be stable. After 180 days of hardening, the maximum contraction strain is  $1.33 \times 10^{-3}$ .

**2.3. The Expansion Strain and Contraction Strain of the Matrix.** The expansion strain and contraction strain of the asphalt matrix can go a long way to influence the internal stresses of the semiflexible pavement and therefore must be accounted for in the study. According to prior research [13], the coefficients of thermal contraction and expansion of AC are nonlinear with temperature, as shown in Table 6.

According to data of Table 6, the largest coefficients of thermal contraction and expansion of AC were determined to be  $31.1$  and  $31.2 \mu\epsilon/^\circ\text{C}$ , respectively. Using the most unfavorable climatic conditions as a reference, the maximum surface temperature difference in Guangdong Province of China is about  $40^\circ\text{C}$  in summer, and the maximum contraction strain and expansion strain of AC may be  $1.24 \times 10^{-3}$  and  $1.25 \times 10^{-3}$ .

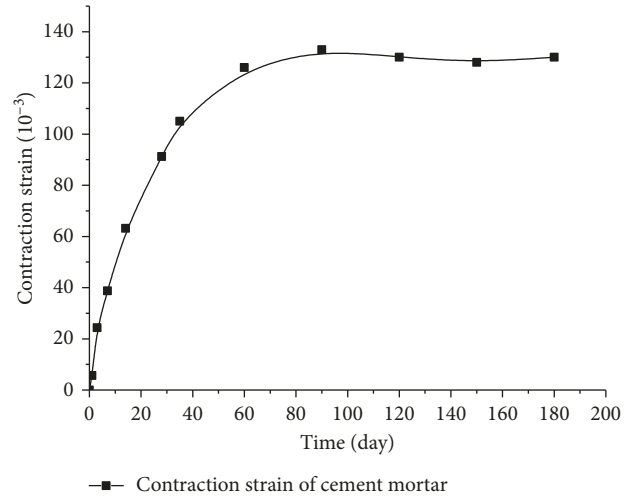


FIGURE 1: Contraction curve of cement mortar.

TABLE 6: Measured coefficients of thermal contraction and expansion at different temperature ranges.

Temperature range ( $^\circ\text{C}$ )	The coefficients of thermal contraction and expansion ( $\mu\epsilon/^\circ\text{C}$ )	
	The coefficient of thermal contraction	The coefficient of thermal expansion
-20 to -5	3.3	31.2
-5 to 10	19.2	28.1
10-25	29.4	23.8
25-40	31.1	25.6
40-55	25.7	26.3

Based on the research results [13], gradation of aggregate and air void of the sample do not affect the coefficients of thermal contraction and expansion significantly. Therefore, the maximum contraction strain and expansion strain of the asphalt matrix are referenced to  $1.24 \times 10^{-3}$  and  $1.25 \times 10^{-3}$  in this paper.

**2.4. Indirect Tensile Test of the Matrix.** This study adopted the multistage aggregate skeleton space-filling method [14, 15] to design the gradation of the matrix under the target air void (15%, 20%, 25%, and 30%) and combined the drainage test and the Cantabro test to determine the optimum asphalt content. The grading design results are shown in Table 7.

The ultimate tensile strength of the matrix is directly related to the cracking resistance of the semiflexible pavement materials. In this study, the MTS testing machine was used for the indirect tensile strength test to measure the indirect tensile strength of the matrix specimens with different air voids. Then, the splitting strength of the matrix would be calculated. This study used the indirect tensile strength of the matrix as the ultimate tensile strength. The ultimate tensile strength of the matrix is shown in Table 8.

TABLE 7: The grading design results of the asphalt mixture matrix with different target air voids.

Sieve size (mm)	Percent passing										Asphalt content (%)	
	19	16	13.2	9.5	2.36	1.18	0.6	0.3	0.15	0.075		
Air voids (%)	15	100	81.9	60.1	29.2	23.6	14.5	13.1	8.6	5.1	3.4	4.6
	20	100	78.7	57.3	25.4	19.4	13.6	12.5	8.4	4.8	3.2	4.2
	25	100	74.1	54.0	17.2	15.1	13.7	11.4	8.2	4.5	3.0	3.8
	30	100	71.4	51.4	15.2	13.7	12.4	10.6	7.6	4.2	2.7	3.4

TABLE 8: Ultimate tensile strength of the matrix.

The air void of the matrix (%)	Ultimate tensile strength of the matrix (MPa)
15	0.36
20	0.34
25	0.31
30	0.28

2.5. *Semiflexible Pavement Molding.* After the specimens were molded, they would be placed statically for 24 hours. The specimens were fixed to the vibration platform, and the cement mortar was poured into the matrix mixture until the surface voids were filled under multiple vibrations. The specimens were then stored in a curing box at constant temperature and humidity (temperature  $20^{\circ}\text{C} \pm 3^{\circ}\text{C}$  and humidity  $>90\%$ ) for 7 days. To identify the grouting depth of cement mortar, a small amount of Sudan dye was added to color the cement mortar.

The voids of the matrix can be divided into closed voids and connected voids. It is difficult to pour cement mortar into the closed voids. In order to ensure the accuracy, the amount of cement mortar grouting would be measured. As shown in the formula (1), the actual air void would be calculated to select the specimens whose actual air void is close to target air void. The density of cement mortar is  $1.87\text{ g/cm}^3$ . The test results are shown in Table 9.

$$V_{\text{actual air void}} = \frac{m}{\rho \times v}, \quad (1)$$

where  $V_{\text{actual air void}}$  is the actual air void of the matrix,  $m$  is the amount of cement mortar grouting quantity,  $\rho$  is the density of cement mortar,  $\rho = 1.87\text{ g/cm}^3$ , and  $v$  is the volume of the specimen.

As shown in Table 9, by comparing the actual air void and target air void, the specimens 15-2, 15-3, 15-4, 20-2, 20-3, 20-6, 25-3, 25-4, 25-5, 30-2, 30-5, and 30-6 were selected for the follow-up study.

2.6. *Finite Element Simulation.* In this study, the semiflexible pavement structure was used as the simulation prototype, and the internal stress of the semiflexible pavement was analyzed by using the two-dimensional plane strain finite element method. The peak stress and stress level of the matrix were calculated considering the expansion and contraction deformations of the cement mortar. Asphalt mixture is a typical viscoelastic material, but in order to simplify the calculation, the linear elastic model is used to characterize the constitutive model of the asphalt mixture matrix and cement mortar in the semiflexible pavement structure. The basic assumptions are as follows:

TABLE 9: The quantity of grout to the asphalt mixture matrix.

Target air void (%)	Specimen number	Cement mortar grouting volume (g)	Actual air void (%)
15	15-1	124.16	13.2
	15-2	133.57	14.2
	15-3	134.51	14.3
	15-4	132.63	14.1
	15-5	126.04	13.4
	15-6	121.34	12.9
20	20-1	171.19	18.2
	20-2	181.54	19.3
	20-3	178.72	19.0
	20-4	167.43	17.8
	20-5	163.67	17.4
	20-6	177.78	18.9
25	25-1	217.28	23.1
	25-2	210.70	22.4
	25-3	225.75	24.0
	25-4	224.81	23.9
	25-5	227.63	24.2
	25-6	216.34	23.0
30	30-1	269.01	28.6
	30-2	273.72	29.1
	30-3	249.26	26.5
	30-4	259.61	27.6
	30-5	272.78	29.0
	30-6	272.78	29.0

- (1) The semiflexible pavement structure consists of the asphalt mixture matrix and cement mortar. The asphalt mixture matrix is a homogeneous and isotropic material.
- (2) As cement mortar and matrix asphalt mixture both produce contraction deformation and expansion deformation, in order to facilitate the finite element calculation, the volume of the matrix asphalt mixture is locked in the finite element model, and the volumetric deformation of cement mortar is defined as the relative volumetric deformation of the matrix asphalt mixture and cement mortar.
- (3) The influence of the road surface weight is not considered.
- (4) The adhesion between matrix and cement mortar is good, without any separation phenomenon.

To obtain a semiflexible pavement cracking resistance model, this study cut semiflexible pavement specimens with different air voids and then used a CCD digital camera to collect the screenshots of the specimens, as shown in Figure 2.

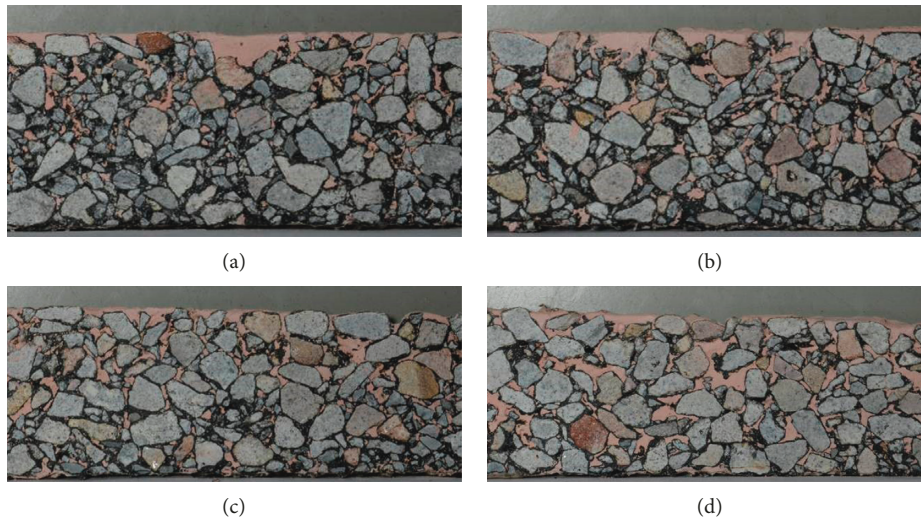


FIGURE 2: Cross-sectional images of semiflexible pavement. (a) 15% air void of the matrix; (b) 20% air void of the matrix; (c) 25% air void of the matrix; (d) 30% air void of the matrix.

The images of the semiflexible pavement were imported into AutoCAD software, and sectional information view was extracted to indicate the distributions of cement mortar, matrix, and air, as shown in Figure 3.

Taking the CAD images of the semiflexible pavement as the calculation model, the CAD images were imported into the finite element software. The material parameters were input, and the contact type was defined. For the boundary conditions, the upper boundary was bounded, the lower boundary was fixed ( $U_1 = UR_1 = UR_2 = 0$ ), the left and right boundaries were horizontally constrained ( $U_1 = UR_1 = UR_2 = 0$ ), the meshing partition was controlled using a triangular element (Tri), and the model had about 300,000 microcells. The meshing partition results are shown in Figure 4.

In Figure 4, the green part represents the aggregate, the white part indicates the cement mortar, and the red part is the asphalt. By changing the expansion and contraction of cement mortar, the stress distributions of aggregate and cement mortar were calculated. Due to the large size of the model, the computation takes a great deal of time. Therefore, five cross sections of each semiflexible pavement material with different air voids would be chosen to calculate the average value.

According to prior research [16–19], the material parameters of the semiflexible pavement were set up using the finite element analysis, as shown in Table 10.

Based on Sections 2.2 and 2.3, the contraction strain and expansion strain range of cement mortar is from  $-1.33 \times 10^{-3}$  to  $1.92 \times 10^{-3}$ , and the contraction strain and expansion strain range of the matrix is from  $-1.24 \times 10^{-3}$  to  $1.25 \times 10^{-3}$ . Therefore, the relative deformation range of the internal structure of the matrix and cement mortar is  $-2.58 \times 10^{-3}$  to  $3.16 \times 10^{-3}$ . In this paper, the volume of the matrix was locked, and the volume deformation rate range of cement mortar during the finite element simulation was set from  $-4 \times 10^{-3}$  to  $4 \times 10^{-3}$ , with an analysis calculation every  $0.5 \times 10^{-3}$ . The peak stress of the matrix was calculated under the conditions of contraction and expansion of the cement mortar.

Taking a 20% air void of the matrix as an example, the finite element analysis charts of the semiflexible pavement are as shown in Figure 5.

### 3. Results and Discussion

**3.1. Stress Peak Analysis.** The finite element simulation results show that the internal stress of the matrix mixture is related to the contraction and expansion deformations of cement mortar, as indicated in Figure 6.

Figure 6 shows the following:

- (1) Contraction and expansion deformations of the cement mortar both produce tensile stress in the matrix. In addition, the stress level of the contraction deformation is significantly higher than that of the expansion deformation. Taking a matrix mixture of 15% air void as an example, when the cement mortar shrinks by 0.2%, the internal stress of the matrix asphalt mixture is 0.46 MPa, but when the cement mortar expands by 0.2%, the internal stress of the matrix asphalt mixture is only 0.16 MPa; that is, the contraction stress is 2.8 times greater than the expansion stress. Meanwhile, the internal stress of the matrix mixture under the contraction of cement mortar grows obviously faster than that under the expansion deformation. It can be seen that the contraction deformation of cement mortar is the dominant factor that affects the stress growth of semiflexible pavement materials. Therefore, if the stress peak of semiflexible pavement is taken as an anticracking indicator, the cement mortar contraction stress should be controlled.
- (2) When the cement mortar expands, the internal stress of the matrix mixture has a good linear relationship with the expansion deformation. When the contraction deformation of the cement mortar is greater than 0.2%, the internal stress and contraction

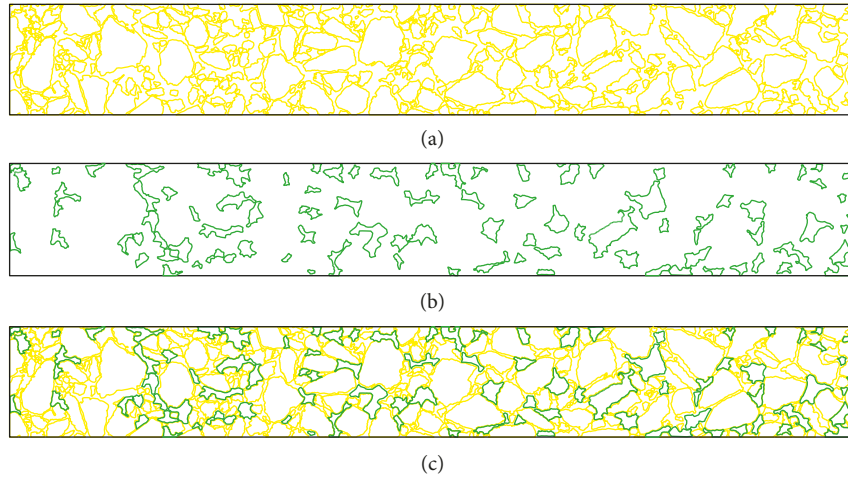


FIGURE 3: Sectional information view of the semiflexible pavement (15% air void). (a) Aggregate distribution; (b) cement mortar distribution; (c) distribution of materials.

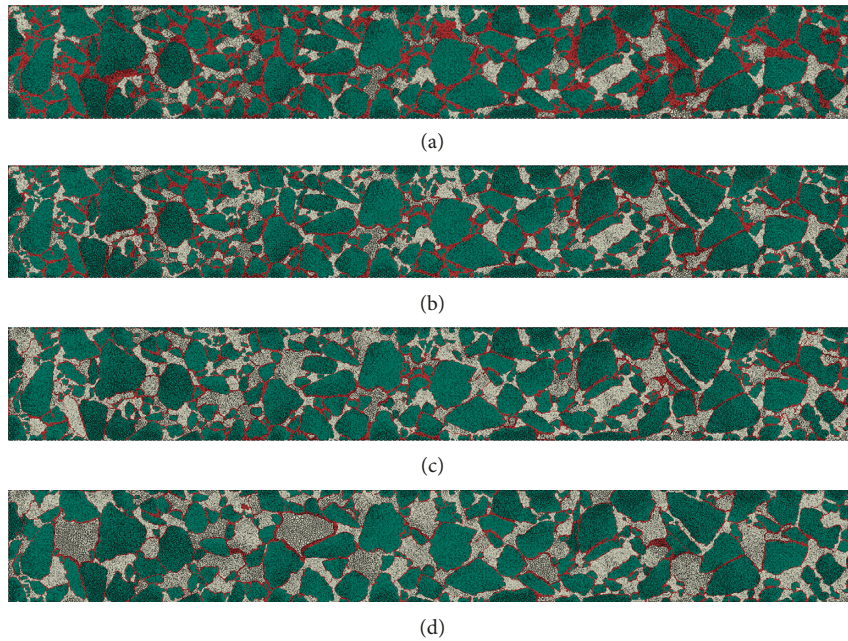


FIGURE 4: Finite element model of the semiflexible pavement. (a) 15% air void of the matrix; (b) 20% air void of the matrix; (c) 25% air void of the matrix; (d) 30% air void of the matrix.

TABLE 10: Material parameters of the semiflexible pavement.

Material	Poisson's ratio	Elastic modulus (MPa)
Asphalt (25°C)	0.35	1250
Aggregate (granite)	0.28	120000
Cement mortar	0.30	15000

deformation of the matrix mixture show a linear growth relationship. When the contraction deformation is less than 0.2%, the internal stress of the matrix mixture is a nonlinear growth model, and the internal stress growth rate decreases with the increase of the deformation amount. It is shown that

the matrix mixture is more sensitive to the change in stress when the contraction of the cement mortar is small.

When the cement mortar shrinks and expands, the relationship between air void of the matrix and stress level is as shown in Figure 7.

It can be seen from Figure 7 that the internal stress of the matrix increases with the increase of the contraction of cement mortar. And the air void of the matrix affects the growth rate of stress. Under the same deformation conditions, the smaller the air void of the matrix mixture is, the greater the stress and stress growth rate is. For example, the stress growth rate is about 1.7 MPa/% for 15% air void of the

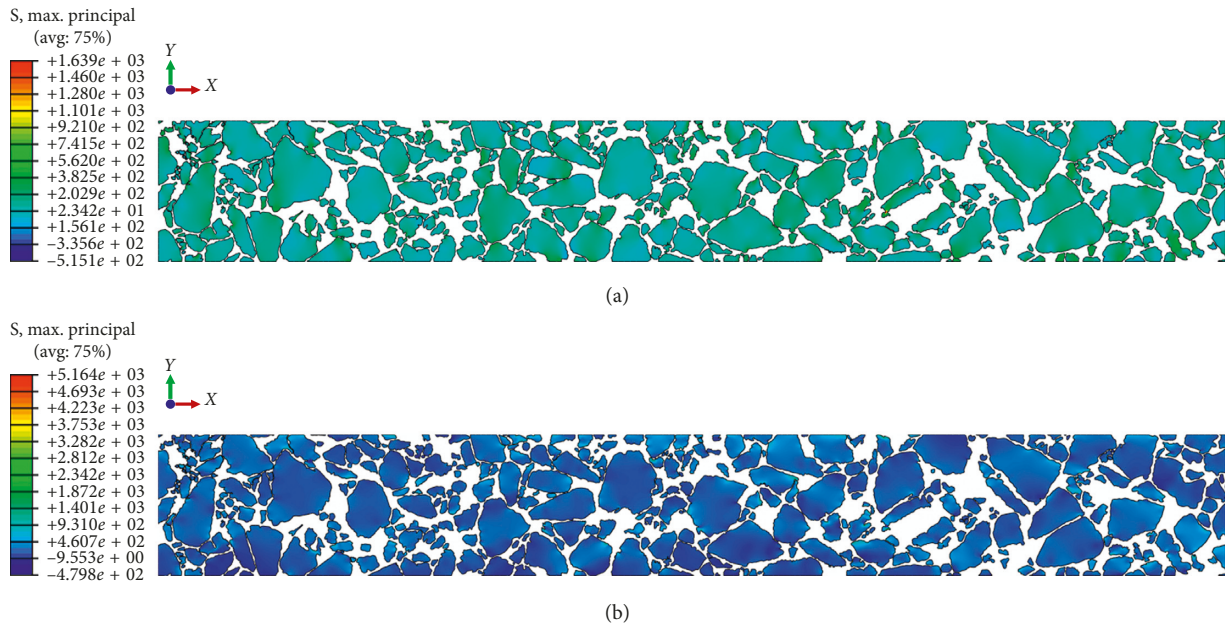


FIGURE 5: Matrix mixture stress cloud. (a) 20% air void, 0.2% expansion; (b) 20% air void, 0.2% contraction.

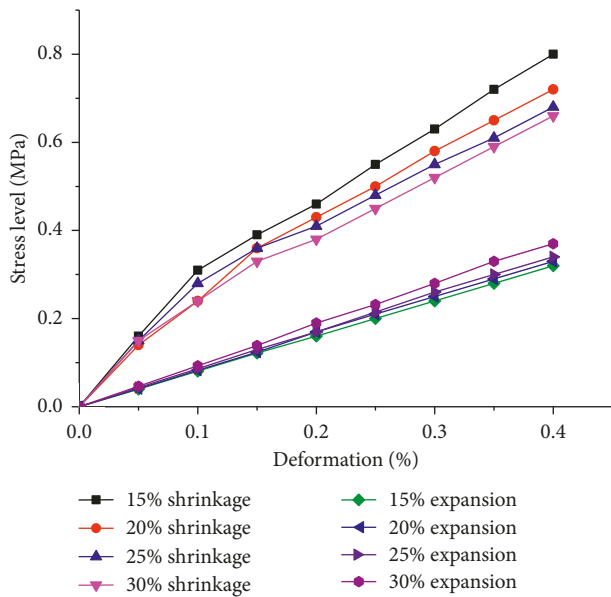


FIGURE 6: The relationship between internal stress of the matrix and deformation of cement mortar.

asphalt mixture matrix, whereas the stress growth rate is 1.3MPa/% for 30% air void of the asphalt mixture matrix. Thus, the lower the air void of the matrix mixture is, the more sensitive the stress generated by the contraction of the cement mortar becomes. It can be seen that an appropriate increase in the air void of the matrix, to a certain extent, can reduce the cracking caused by the contraction of cement mortar.

In contrast with the contraction of cement mortar, the larger the air void of the matrix mixture is, the higher the internal stress level under an expansion deformation

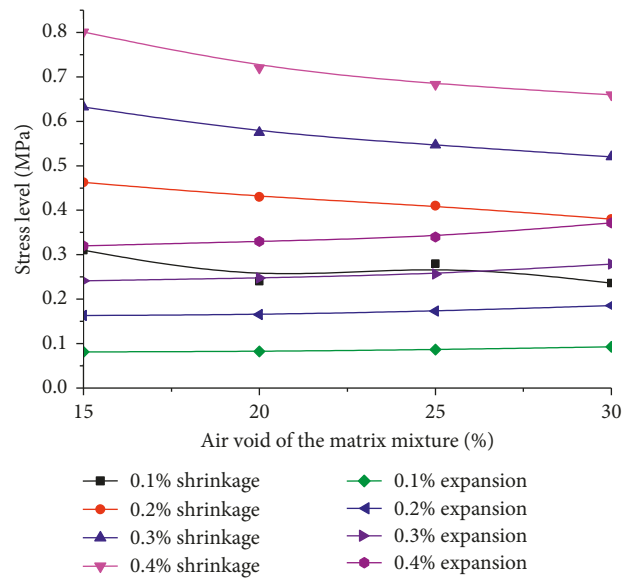


FIGURE 7: Relationship between air void and stress of the asphalt mixture matrix.

becomes. In addition, the internal stress produced by expansion deformation is much lower than that by contraction deformation. When the air void of the matrix is between 15% and 25%, the internal stress under the same deformation is basically the same. When the air void of the matrix asphalt mixture is more than 25%, the internal stress of the matrix mixture slowly increases. In general, an increase in the air void of the matrix has little effect on the internal stress growth caused by expansion deformation.

According to the analysis above, larger air void of matrix asphalt structure and less volumetric variation of cement mortar reduce the internal stress. In the actual

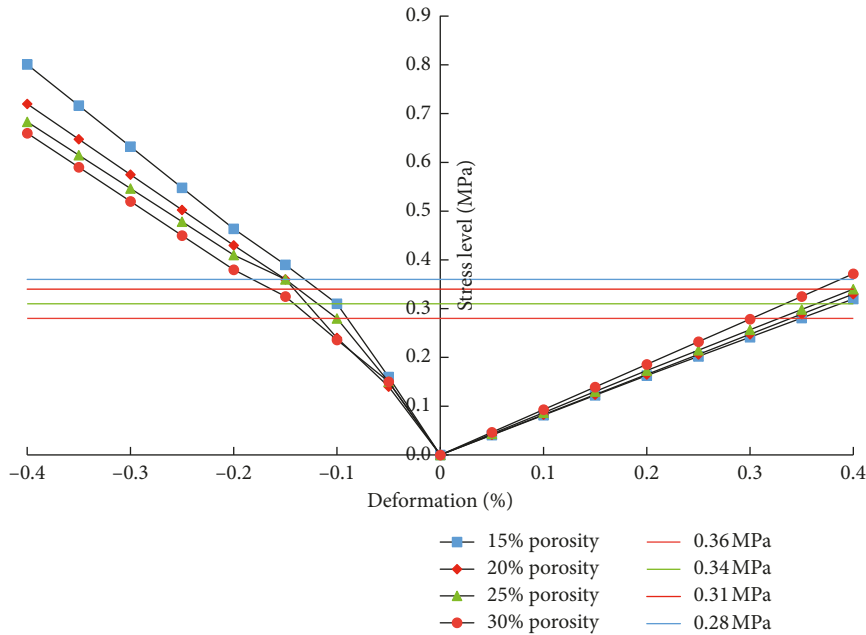


FIGURE 8: Relationship between stress and deformation of the matrix mixture.

project, after measuring the ultimate tensile strength of matrix asphalt structure with target air void, the cement mortar with suitable volume stability can be selected by the peak stress.

**3.2. Strain Control Analysis of Cement Mortar.** As a prerequisite for the anticracking design of semiflexible pavement materials, the contraction stress and expansion stress of cement mortar should be less than the ultimate tensile strength of the matrix asphalt mixture. Therefore, a threshold value of stress can be set to control the peak stress of cement mortar. As described in Table 7, the threshold value of the ultimate deformation of the cement mortar can be obtained by controlling the ultimate tensile strength of the matrix mixture. When the deformation is negative, it indicates a contraction deformation of the cement mortar, whereas a positive value indicates an expansion deformation.

The relationship between the stress curve caused by the contraction and expansion deformations of cement mortar under different air voids and the corresponding ultimate tensile strength is shown in Figure 8. The results calculated by the interpolation method show that when the air void of the matrix mixture is 15%, the maximum contraction of cement mortar should be less than 0.13%, and the maximum expansion should be less than 0.4%. When the air void of the matrix is 20%, the maximum contraction of cement mortar should be less than 0.14%, and the maximum expansion should be less than 0.4%. When the air void is 25%, the maximum contraction of cement mortar should be less than 0.12%, and the maximum expansion should be less than 0.38%. When the air void is 30%, the maximum contraction should be less than 0.12%, and the maximum expansion should be less than 0.31%.

Therefore, for the matrix and cement mortar used in this paper, the maximum allowable deformation values of cement mortar are summarized in Table 11.

According to the above analysis, this study proposes an anticracking design method of semiflexible pavement materials. Firstly, the ultimate tensile strength of matrix asphalt structure with target air void is measured, and the results are input into a mechanical model for numerical simulation to determine the maximum allowable strain of cement mortar. To avoid the cracking of semiflexible pavement, cement mortar whose maximum contraction strain and expansion strain are both below the maximum allowable strain is selected to alleviate the internal cracking concern of the semiflexible mixture.

## 4. Conclusions

This study proposed an anticracking design method of semiflexible pavement materials. The ultimate tensile strength of matrix asphalt structure with target air void was measured, and the results were input into a mechanical model for numerical simulation to determine the maximum allowable strain of cement mortar. Based on the laboratory test results and FEM simulation, the following findings were obtained:

- (1) Both contraction and expansion deformations of cement mortar produce tensile stress in the asphalt mixture matrix. The stress of cement mortar from contraction deformation is significantly higher than that from expansion deformation. The contraction deformation of cement mortar is the dominant factor causing internal stress in semiflexible pavement. In addition, the matrix mixture is more sensitive to the changes in stress when the less contraction deformation of the cement mortar occurs.

TABLE 11: The maximum allowable deformation values of cement mortar.

The air void of the matrix (%)	Maximum allowable contraction (%)	Maximum allowable expansion (%)
15	0.13	0.40
20	0.14	0.40
25	0.12	0.38
30	0.12	0.31

- (2) The expansion deformation of cement mortar shows a good linear relationship with the internal stress of the matrix, and the tensile stress produced by the expansion of cement mortar is much lower than that caused by contraction. In addition, the increase in air void of the matrix has little effect on the internal stress growth caused by expansion deformation.
- (3) Larger air void of matrix asphalt structure and less volumetric variation of cement mortar reduce the internal stress. For real projects, the ultimate tensile strength of the matrix with target air void can be measured and the peak stress can be used as the control index to select cement mortar with suitable volume stability.

This paper mainly puts forward the research method of semiflexible pavement internal crack resistance. As the deformation of asphalt matrix and cement mortar changes dynamically with temperature and time, and the variation trend is different, the relative deformation of cement mortar and asphalt matrix considered in this paper is not very accurate. In future research, the expansion strain and contraction strain-time curve of cement mortar and asphalt matrix will be further studied, and the expansion and contraction deformations of cement mortar and asphalt matrix will be simulated by the finite element method, and the stress change of semiflexible pavement internal structure will be accurately calculated.

## Data Availability

No data were used to support this study.

## Conflicts of Interest

The authors declare that there are no conflicts of interest regarding the publication of this paper.

## Acknowledgments

The authors sincerely acknowledge the funding support from the National Natural Science Foundation of China (NSFC 51808228) and the Fundamental Research Funds for the Central Universities (2018MS92).

## References

- [1] C. Pratelli, G. Betti, T. Giuffrè, and A. Marradi, "Preliminary in-situ evaluation of an innovative, semi-flexible pavement wearing course mixture using fast falling weight deflectionometer," *Materials*, vol. 11, no. 4, p. 611, 2018.
- [2] G. Berardi and P. Di Mascio, "Le pavimentazioni aeroportuali in conglomerato bituminoso open grade intasato di Malta cementizia-open grade asphalt concrete filled with cement mortar for airport pavements," *Rassegna del Bitume*, vol. 61, pp. 29–36, 2009.
- [3] S. E. Zoorob, K. E. Hassan, and A. Setyawan, "Cold mix, cold laid semi-flexible Grouted Macadams mix design and properties," in *Proceedings of the Performance of Bituminous and Hydraulic Materials in Pavements*, CRC Press, Nottingham, UK, April 2002.
- [4] K. E. Hassan, A. Setyawan, and S. E. Zoorob, "Effect of cementitious grouts on the properties of semi-flexible bituminous pavements," in *Proceedings of the Performance of Bituminous and Hydraulic Materials in Pavements*, CRC Press, Nottingham, UK, April 2002.
- [5] D. V. Ramsamooj, J. Ramadan, and G. S. Lin, "Model prediction of rutting in asphalt concrete," *Journal of Transportation Engineering*, vol. 124, no. 5, pp. 448–456, 1998.
- [6] I. J. Huddleston, H. Zhou, and R. G. Hicks, "Evaluation of open-graded asphalt concrete mixtures used in Oregon," Transportation Research Record 1427TRB, National Research Council, Washington, DC, USA, 1993.
- [7] C. Huang, "Study on volume stability and crack resistance of semi-flexible pavement," M.S. thesis, Wuhan University of Technology, Wuhan, China, 2010.
- [8] W. Wang and K. Wu, "Study on crack resistance of semi-flexible pavement based on J-integral," *Highway*, vol. 61, no. 11, pp. 63–66, 2016.
- [9] C. Huang, J. P. Liu, J. X. Hong, and Z. F. Liu, "Improvement on the crack resistance property of semi-flexible pavement by cement-emulsified asphalt mortar," *Key Engineering Materials*, vol. 509, pp. 26–32, 2012.
- [10] Japan Association of Roads, *Explain for General Code of Asphalt Pavement Engineering*, Maruzen Co., Ltd., Tokyo, Japan, 1992.
- [11] D. Shen, J. Shen, J. Huang et al., "Study on thermal expansion coefficient of cement - based materials in early age and hardening stage," *Journal of Hydraulic Engineering*, vol. 43, no. 1, pp. 153–160, 2012.
- [12] S. Li, "Cement mortar contraction research," M.S. thesis, Nanjing University of Technology, Nanjing, China, 2004.
- [13] M. R. Islam and R. A. Tarefder, "Coefficients of thermal contraction and expansion of asphalt concrete in the laboratory," *Journal of Materials in Civil Engineering*, vol. 27, no. 11, article 04015020, 2015.
- [14] G. Lees, "The rational design of aggregate gradings for dense asphaltic compositions," in *Proceedings of Asphalt Paving Technologies*, pp. 60–90, Kansas City, MO, USA, 1970.
- [15] X. Cai, D. Wang, K. Wu, and G. Yang, "Design of anti-rutting asphalt mixture by simplified classification method," *Journal of Highway and Transportation Research and Development*, vol. 33, no. 3, pp. 13–17, 2016.
- [16] A. Epps, T. Ahmed, D. C. Little et al., "Performance assessment with the MMLS3 at WesTrack," *Asphalt Paving Technology: Association of Asphalt Paving Technologists Proceedings of the Technical Sessions*, vol. 70, pp. 509–542, 2002.
- [17] R. B. Mallick and J. A. Bergendahl, *An Evaluation of Rutting and Shoving Potential of, and Chloride Diffusion through Hot Mix Asphalt (HMA) with Rosphalt*, Civil and Environmental

Engineering Department, Worcester Polytechnic Institute,  
Worcester, MA, USA, 2004.

- [18] L. Shao, S. Chi, and Y. Jia, "Mesoscopic simulation of large triaxial test of rockfill material," *Rock and Soil Mechanics*, vol. 30, no. S1, pp. 239–243, 2009.
- [19] X. Shao, M. Shao, Y. Bi et al., "Asphalt mixture Poisson's ratio test method," *Journal of Tongji University (Natural Science Edition)*, vol. 34, no. 11, pp. 1470–1474, 2006.

